Multidisciplinary investigation of active shallow pockmarks in Dunmanus Bay.

Dublin City University

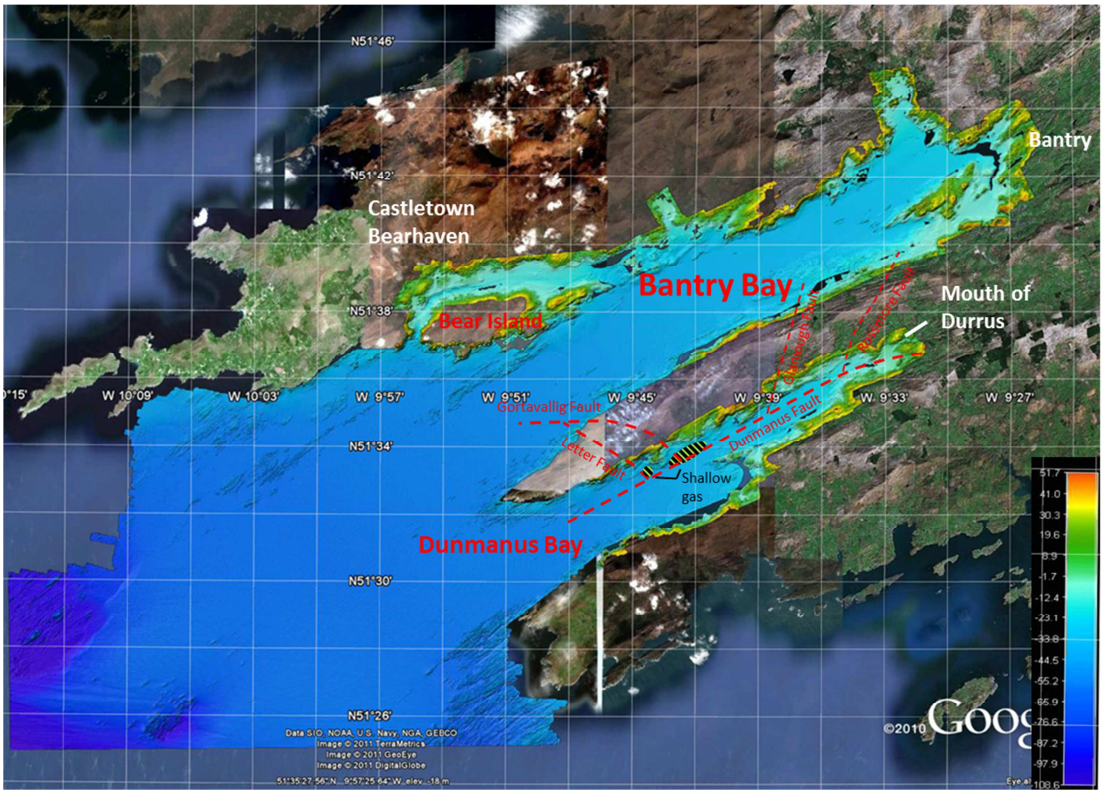

Report for the Petroleum Infrastructure Programme (PIP), 2014

Contributors: Shane O' Reilly, Brian Kelleher (DCU)[1]
Michal Szpak (DCU)[1] and Xavier Monteys (GSI)[2]

1. School of Chemical Sciences, Dublin City University, Glasnevin, Dublin 9
2. Geological Survey of Ireland, Beggars Bush, Haddington Road, Dublin 4
** Correspondence to brian.kelleher@dcu.ie*

Table of contents

1 Introduction

Pockmarks are circular or sub-circular seabed depressions, which may reach diameters of hundreds of metres and depths of tens of metres (Judd and Hovland 2007). They occur in a variety of settings, which include estuaries (Garcia-Gil et al., 2003; Garcia-Gil 2003) shallow bays (Knebel and Scanlon 1985; Kelley et al., 1994; Ussler et al., 2003), continental shelves (Nelson et al., 1979;Fader 1991), continental slopes and rises (Paull et al., 2002; Gay et al., 2006), and lakes (Pickrill 2006). Sub-seabed fluid escape is usually invoked as the primary formation mechanism for these features, and the current leading formation theory was proposed by (Hovland and Judd 1988). This includes three primary stages: (1) the formation of a seabed dome due to excessive fluid pressure underneath the seabed; (2) discharge of the fluid in a single event, expelling the sediment into the water column, winnowing fine-grained sediment and leaving lag deposits; and (3) continuation of pockmark formation due to continual or episodic seepage. Thus lithology is thought to be one of the primary parameters for pockmark occurrence, since fine-grained clay/silt has a lower permeability than coarser grains and hence facilitate gas accumulation and overpressurisation. The main associated fluid is gas, which may be thermogenic or microbial gas from organic-rich sedimentary deposits (Judd and Hovland 2007). Frequently however, surveyed pockmarks are not associated with evidence, be that geophysical or geochemical, of gas (or other fluids) migration and are deemed inactive or that another formation mechanism may be possible (Paull et al., 2002; Ussler et al., 2003; Rogers et al., 2006). Alternative pockmark formation theories inlcude pore water escape (Harrington 1985), fresh/groundwater seepage (Whiticar 2002; Christodolou et al., 2003), ice-rafting (Paull et al., 1999), biological activity and meteorite impacts (Judd and Hovland 2007). Thus significant questions remain regarding pockmark formation, distribution and processes.

To date there have been few studies of biological productivity associated with pockmarks and most have focused on macrofaunal assemblages present (Dando 1991; Ondreas et al., 2005; Judd and Hovland 2007; Webb et al., 2009). In contrast to active deep sea sites, biological productivity at shallow pockmarks settings does not seem to be very different from surrounding sediment. Studies of microbial diversity in pockmarks have reported microbes known to be involved in the anaerobic oxidation of methane (AOM), similar to other cold seep features with moderate/high CH_4 flux.

(Wegener et al., 2008; Boulabassi et al., 2009; Cambon-Bonavita et al., 2009; Merkel et al., 2010; Shubenvova et al., 2010; Roalkvam et al., 2011, 2012). However at present little is known about the effect of pockmark formation and seepage processes on microbial communities, and vice-versa about the role, if any, is played by microbes in pockmarks formation and seepage.

A pockmark field was discovered in Dunmanus Bay, south west Ireland, in 2007 during multibeam mapping of the bay in shallow water depths of about 40 m. Over 60 pockmarks have been mapped that reach a maximum diameter of 20 m, do not appear to exceed 1 m in depth. These pockmarks occur in clusters, possibly comprising composite features, and also small (1 to 2 m diameter) satellite features. The lithology of the bay is dominated by coarse to medium sand, while mud to fine sand is dominant closer to the mouth of the bay. The Dunmanus Bay pockmark field (DBPF) is coincident with an area of comparatively finer particle size (Szpak 2012a). Initial surveys highlighted that acoustic evidence of minor subsurface gas seepage is widespread across the region. However regions of shallow (< 10 mbsf) acoustic turbidity (AT), indicating gas accumulations, are coincident with fine-grained muddy seabed occurring in the mapped pockmark field. Furthermore the DBPF coincides of subtle water column acoustic echofacies, indicating low to moderate fluid seepage is occurring (Szpak 2012a). A number of faults bisect and cross the region, and are thought to be likely routes of gas migration to shallow sediments.

However the exact nature of the seeping fluid, its relationship with seabed lithology and the key biogeochemical processes occurring at this site have not been studied comprehensively and are poorly understood at present. The purpose of this study was to conduct a geochemical and microbiological investigation of pockmarked and non-pockmarked sediment within DBPF, and surrounding sediments in order to elucidate distinct chemical and physical processes within the pockmark field.

2 Materials and Methods

2.1 Environmental and Geological Setting

Dunmanus Bay is located in southwest Ireland, between the Sheep's Head and Mizen peninsulas (Fig. 2.1). The bay is nearly 7 km wide at its widest point and 22 km long. The Durrus River drains into the bay at Durrus. INFOMAR surveys aboard the RV Celtic Explorer mapped the outer region of Dunmanus Bay in 2006, followed by the

intermediate depths in 2007 (RV Celtic Voyager). A Tenix LADS lidar survey was also conducted in 2006 and mapped the nearshore and shallow waters of the bay. Water depths range from 0 to 70 m to the southwest at the mouth of the bay. Dunmanus Bay lies in the South Munster Basin. The Dunmanus Fault runs along the centre of the Bay parallel to the landmass, whereby two minor faults, the Gortavallig Fault and the Letter Fault, occur perpendicular to the Dunmanus Fault in the vicinity of the pockmark field (Szpak 2012a). Two other notable faults to the north west are the Rossmore Fault and the Glanlough Fault (MacCarthy 2007). The northern part of the bay is dominated by coarse to medium sand, while mud to fine sand is dominant closer to the mouth of the bay. Localised occurrences of rock outcroppings and gravels also occur, and generally in proximity to the landmasses. Quaternary sediment thickness does not generally exceed 22 m (Monteys et al., 2010). The DBPF consists of an area of seabed of approximately 222000 km^2 and is located in proximity to the landmass (620m east of Dooneen Point) in about 40 m water depth. Seabed in this area is dominated by mud to fine sand. For an in-depth discussion of the geological and environmental setting of Dunmanus Bay, see Szpak (2012a).

2.2 Core sampling

Sediment vibrocores were sampled using a GeoResources Geo-Corer 6000. Cut and capped core sections were split and archive halves photographed and logged. Sediment sub-samples were taken from working sections after gas and pore water sampling (see section 2.2.3), and stored onboard at -20^oC, and at -80^oC back in the laboratory. Sub-samples for bulk chemical and physical parameters were stored at 4^oC.

2.3 Gas and pore water analysis

Interstitial gas sampling was carried out immediately upon core retrieval. 10 mL sediment plugs were sampled from windows cut in the core liner, transferred to a 20 mL headspace vial and 1.2 M NaCl solution containing approximately 70 mg L^{-1} thimerosal (Sigma Aldrich, Dorset, UK) was then added to the vial leaving a 3 mL headspace. Sealed vials were stored in the dark at 4^oC prior to analysis. CH_4 analysis was performed according on an Agilent 7820A GC-FID with a 30 m HP-PLOTQ column (Agilent, Santa Clara, USA). Column conditions were isothermal (20^oC). CH_4 was quantified using calibration standards prepared from a 99.992% CH_4 standard

(Sigma Aldrich, Dorset, UK). Sediment pore water was sub-sampled from core liner windows using Rhizon samplers (Rhizosphere Research Products, Wageningen, NL). 1 mL aliquots for H_2S analysis were preserved by addition of 400 µL 20 mM zinc acetate. Aliquots for PO_4^{3-} and NH_4^+ analysis were preserved with 1-2 drops of chloroform. Spectrophotometric analysis of H_2S and PO_4^{3-} was performed using leucomethylene blue and phosphomolybdate complexation respectively (Grasshoff et al., 1983). Analysis was conducted on a BIOTEK Powerwave HT plate reader and calibration standards were prepared in artificial seawater prepared from commercially available sea salts (Sigma Aldrich, Dorset, UK). NH_4^+ analysis was performed using a SCHOTT NH1100 ion selective electrode and using NH_3 ISE ion strength adjustment buffer and NH_3 ISE calibration solution (Reagecon, Clare, Ireland). Calibration and quantification was performed according to manufacturer guidelines. SO_4^{2-} and Cl^- anions were determined by suppressed ion chromatography on a DX-120 Dionex Ion Chromatograph with an eluent generator (K_2CO_3). Separation was achieved on a chromatographic system composed of an anion exchange column (IonPak C_{18}) and a guard column. The mobile phase was Nanopure grade water (18MΩ), which was automatically amended with hydroxide ions to a preset concentration (12 mM of OH^-). The mobile phase flow was set to 1.0 ml min^{-1} and suppressor current was set to 22 mA. Data processing and peaks integration was conducted using the Chromelion software package.

2.4 Multi sensor core logger (MSCL)

Duplicate cores from each station were scanned using a GEOTEK MSCL-S multi sensor core logger. Cores were scanned in split mode and bulk density, magnetic susceptibility, P-wave velocity, electrical resistivity, fractional porosity and colour parameters were determined. Scanning was conducted at a resolution of 1 cm^{-1} after calibration according to manufacturer's guidelines (GEOTEK, Daventry, UK). Data was processed using GEOTEK MSCL software (Ver. 7.92.4).

2.2 Bulk chemical and physical analysis

Particle size analysis was performed using laser granulometry (Malvern MS2000) for sediment fractions <1000 µm and dry sieving for fractions >1000 µm. Percentage per size class calculated using the MS2000 were converted to total sample percentages and integrated with the >1000 µm data. Total organic carbon and total nitrogen was

analysed using an Exeter Analytical CE440 elemental analyser, after oven-drying and removal of inorganic carbonate using 1M HCl. Loss-on-ignition (LOI) was determined in higher resolution by combusting 300 to 200 mg oven-dried sediment to constant weight at 440^{o}C for 8 hours in a muffle furnace.

2.6 DNA extraction, PCR and DGGE

DNA was extracted using the POWERSOIL DNA isolation kit (MO BIO, Carlsbad, US) according to manufacturer guidelines. Bacterial and archaeal 16S rRNA PCR and DGGE was performed as outlined previously (see Chapter 3).

2.7 Sedimentary organic matter composition

Sediment OM was isolated according to previously described methods (Gonçalves et al., 2003; Szpak et al., 2012b). Freeze-dried sediment (~120 g accurately weighed) was extracted with deionised water (x3). OM was concentrated and ferromagnetic minerals removed by shaking samples overnight in 10% 1:1 (v/v) HCl/HF (x2), followed by 10% HF (x8). Concentrated OM was then exhaustively extracted with 0.1 M NaOH. Water and NaOH extracts were centrifuged and supernatants were filtered through 0.22 μm polyvinylidene fluoride membrane filters (Merck Millipore, Billerica, USA). Water extracts were combined and dried by rotary evaporation and stored at -80^{o}C. NaOH extracts were ion-exchanged using AMBERJET 1200H cation exchange resin to remove Na^{+} ions. NaOH extracts were subsequently freeze-dried and all extracts were desiccated for 48 hr prior to further analysis.

Each sample (40 mg) was resuspended in 1 mL of D_2O and titrated to pH 13 using NaOD (40% by wt) to ensure complete solubility. Samples were analysed using a Bruker Avance 200MHz NMR spectrometer equipped with a ^{1}H–^{19}F–^{13}C–^{12}N 2mm, quadrupole resonance inverse probe (QXI) fitted with an actively shielded Z gradient. 1-D solution state ^{1}H NMR experiments were performed at a temperature of 298 K with 128 scans, a recycle delay of 3 s, 16384 time domain points, and an acquisition time of 0.8 s. Solvent suppression was achieved by presaturation utilizing relaxation gradients and echoes (Simpson and Brown 2002). Spectra were apodised through multiplication with an exponential decay corresponding to 1-Hz line broadening, and a zero-filling factor of 2. Diffusion-edited (DE) experiments were performed using a bipolar pulse longitudinal encode-decode sequence (Wu et al., 1992). Scans (1024) were collected using a 1.22 ms, 22.2 gauss cm^{-1}, sine-shaped gradient pulse, a

diffusion time of 100 ms, 16384 time domain points and 819 ms acquisition time. Spectra were apodised through multiplication with an exponential decay corresponding to 10 Hz line broadening and zero-filling factor of 2.

2.8 Porewater dissolved organic matter

At least 10 mL aliquots of selected porewater samples were additionally filtered through 0.22 μm PVDF membrane filters and dissolved organic matter (DOM) was subsequently preserved in sodium azide (final concentration of 0.1 %). All NMR experiments were carried out according to Lam and Simpson (2007) on a Bruker Avance 200 MHz equipped with a 2 mm ^{1}H-BB-^{13}C TBI probe with an actively shielded Z-gradient. 1D solution state 1H NMR experiments were acquired with a recycle delay of 2 s, and 32768 time domain points. Spectra were apodized by multiplication with an exponential decay producing a 10 Hz line broadening in the transformed spectrum, and a zero-filling factor of 2. Where appropriate, pre-saturation was applied on resonance generated by a 60 W amplifier attenuated at 20 dB during the relaxation delay. Direct ^{1}H NMR was performed using WATER suppression by GrAdient-Tailored Excitation (WATERGATE) and was carried out using a W2 train and a 122 μs binomial delay such that the 'sidebands' occurred at ca. 12 ppm and 2 ppm and were outside the spectral window. W2-WATERGATE was preceded by a train of selective pulses: 2000, 2 ms, calibrated π (180^{o}) pulses were used, each separated by a 4 μs delay.

2.9 Lipid biomarker analysis

Freeze-dried powdered samples were extracted by a modified Bligh-Dyer method (White and Ringelberg 1998) as described previously. Desulphurised TLE's were fractionated and phospolipid fatty acids analysed as described previosuly (See Chapter 2).

2.10 Biomarker and DGGE data analysis and statistical treatment

Hierarchical cluster analysis of PLFA data was performed using the software PAST (v1.72) (Hammer et al. 2001), using the Bray-Curtis similarity matrix. DGGE gels were digitised and subjected to hierarchical cluster analysis after background subtraction and band matching using the Phoretix 1D gel analysis software (Total Labs Inc., Newcastle, UK).

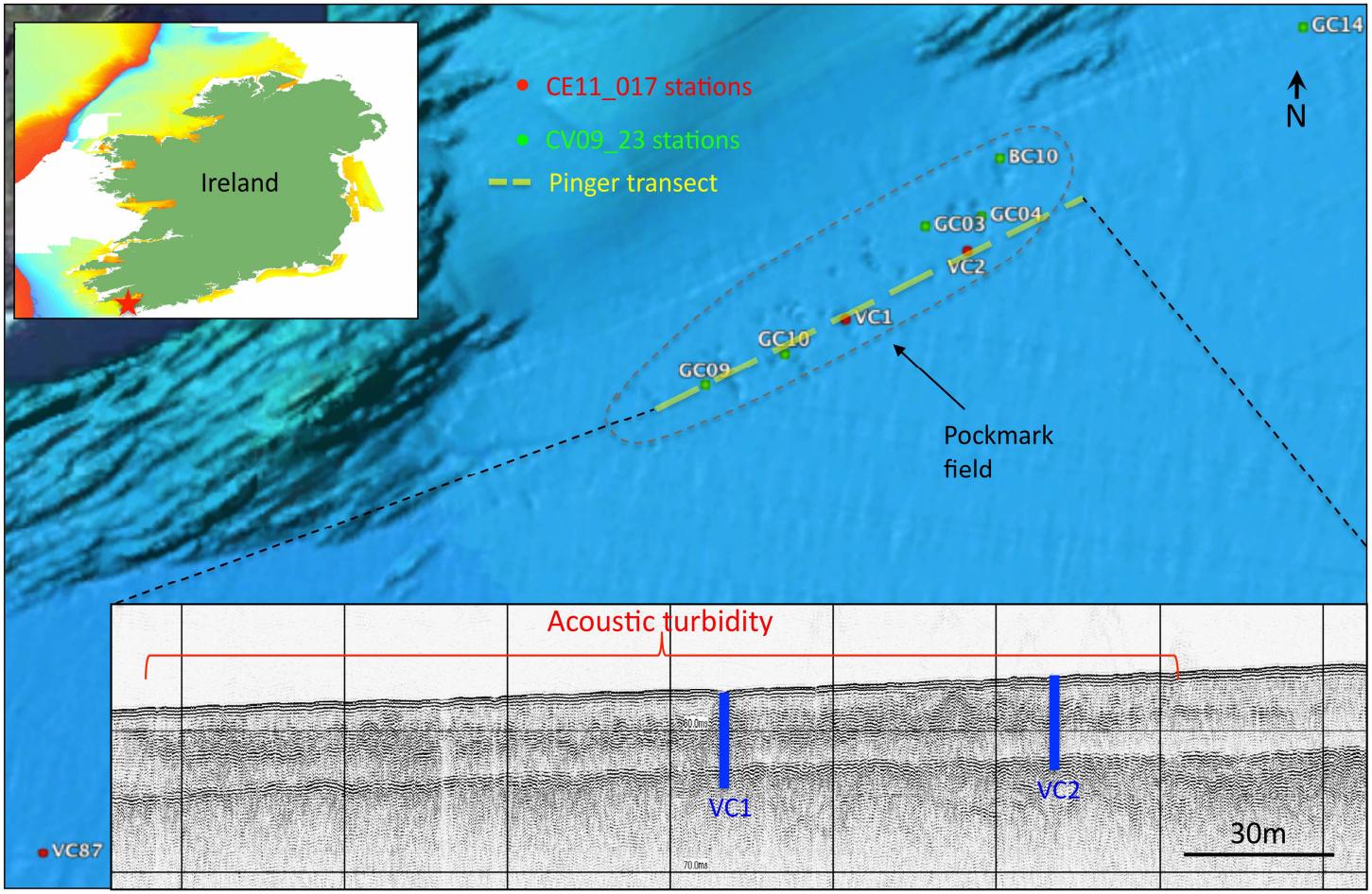

Figure 1: Map showing location of Dunmanus Bay (inset) and bathymetric map of Dunmanus Bay showing location and outline of Dunmanus Bay pockmark field. Sampling stations for the 2009 and 2011 surveys are shown. Inset: Sub-bottom pinger profile showing a transect across the Dunmanus Bay pockmark field. Acoustic turbidity, providing indirect evidence of gas accumulations, is evident and coincident with the pockmark field.

3 Results and Discussion

3.1 Dunmnaus Bay Pockmark field: Lithological control on pockmark formation and geochemical processes?

Downcore physical and chemical profiles for cores VC1, VC2 and VC3 are shown in Fig. 2.2, 2.3 and 2.4, respectively. Specifically sediment class (based on percentage silt, clay and sand composition), bulk organic matter content (expressed as percentage loss-on-ignition), interstitial CH_4, SO_4^{2-}, H_2S, PO_4^{3-}, NH_4^+ and sediment porosity are given. Surface sediments in VC1 from 0 to 1.4 mbsf were characterised by poorly sorted mud, with silt and clay averaging 74.2% and 12.7%, respectively. From 1.4 to 1.6 mbsf sediment is characterised by very poorly sorted muddy sand to sandy mud, followed by a transition to poorly sorted/very poorly sorted sandy mud to 3.0 mbsf. Between 3.0 to 3.8 mbsf there is a gradual transition from sandy mud to muddy sand, followed by a sharp contact and a transition from sandy gravel to coarse gravel until about 4.2 mbsf. From 4.2 mbsf until 2.62 mbsf sediment consists of primarily well sorted sand. VC2 exhibits a lower clay content, higher sand content, and overall a more variable lithology in the first 2 mbsf compared to VC1. Below about 1.8 mbsf sediment type is comparable between VC1 and VC2 (Fig. 4). In contrast, the reference core VC3 displays a more homogeneous lithology over the 2.72 mbsf. Sediment porosity for both VC1 and VC2 was relatively low close to the SWI (~0.4), while the presence of a high porosity layer in the first 12 cm of VC3 was observed (Fig. 2.4). In all 3 cores a distinct gravel stratum was observed at about 4 mbsf. This has been identified as the source of the enhanced reflector in acoustic profiles (Fig. 2.1). Sandy sediments (and indeed gravels) are characterized by a relatively high permeability compared to mud (Wilson et al., 2008). Thus the lithology within DBPF is likely a significant factor controlling the occurrence pockmarks withing this region and not surrounding coarser-grained sediment types. Gas migration via permeable strata and accumulation in muddy layers and eventual expulsion via fluidisation of gas, water and sediment into the water column, as proposed by Judd and Hovland (1988), is thus most likely formation mechanism for pockmarks in Dunmanus Bay.

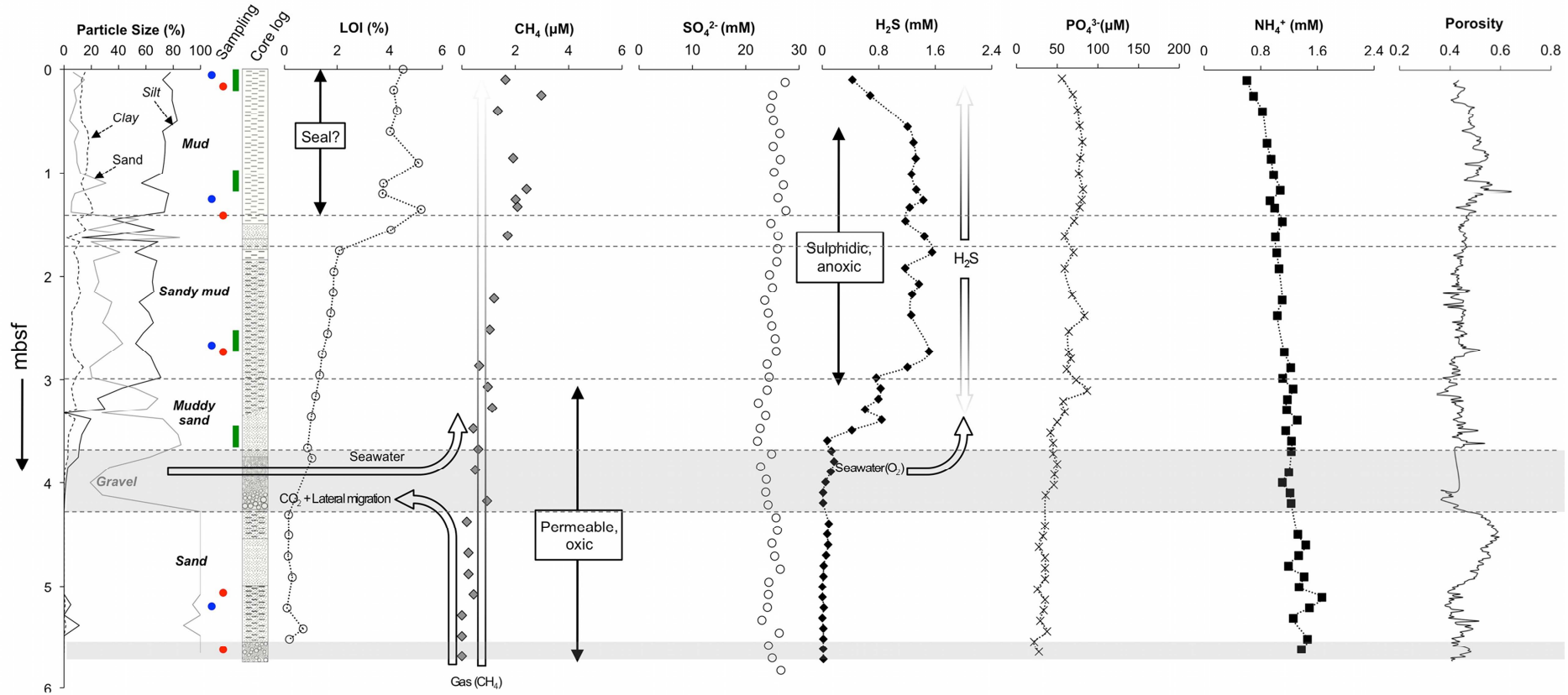

Figure 2: Downcore profiles of physical and chemical parameters from core VC1, sampled from within a pockmark cluster.

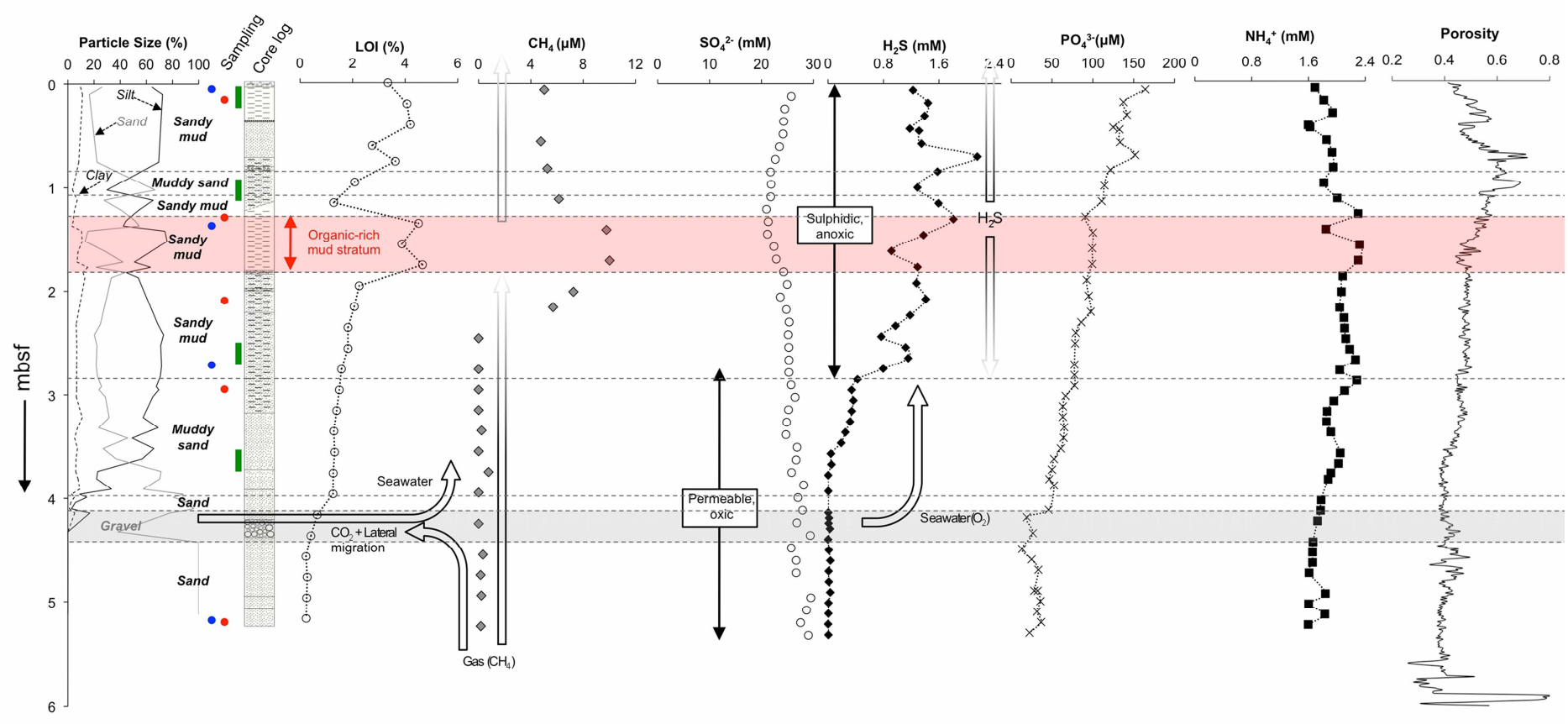

Figure 3: Downcore profiles of physical and chemical parameters from core VC2, sampled from acoustically-turbid non-pockmarked sediment within the Dunmanus Bay pockmark field

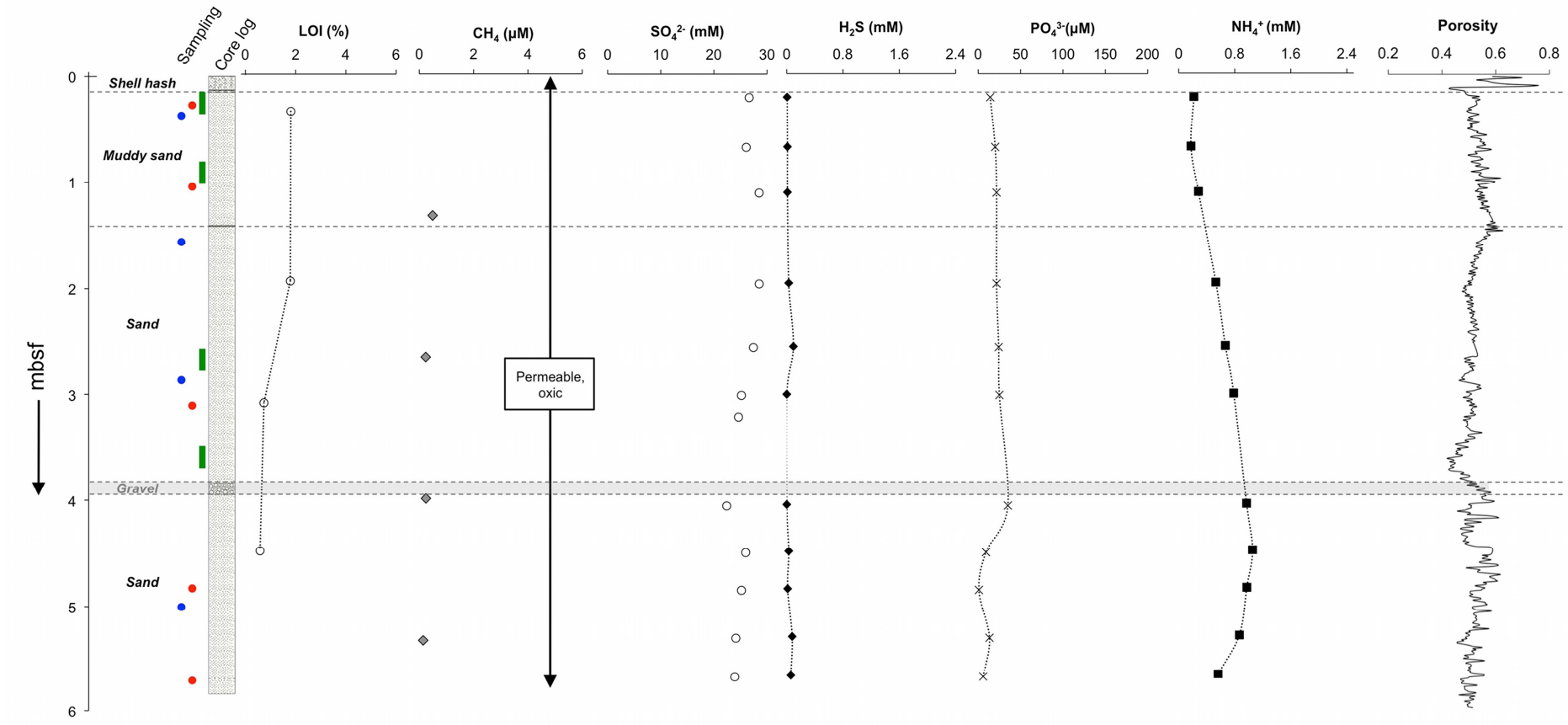

Figure 4: Downcore profiles of physical and chemical parameters from core VC3, sampled from representative sandy sediment in Dunmanus Bay.

Porewater advection through permeable sediments facilitates significant sediment-water exchange of solutes and particles between sediment and the water column (Huettel et al., 1998, 2003; Huettel and Rusch 2000). In this way permeable sands can be major controlling factors on the biogeochemistry of sediments (Santos et al., 2011, and references therein) and biogeochemical cycling can be as high or even higher than organic-rich muddy sediment types (Boudreau et al., 2001). This appears to be reflected in the pore water geochemistry, whereby H_2S concentrations were high in muddy strata in both VC1 and VC2, but rapidly depleted in deeper sediments with coarser sediment type. Concentrations up to 1.22 and 2.12 mM were measured, respectively in muddy strata. In VC1 H_2S increased linearly from less than 0.3 mM to 1.29 mM at 0.70 mbsf. An approximate plateau follows this until 2.82 mbsf, followed by a sharp decrease to negligible concentrations at 3.22 mbsf. This trend was also observed in VC2, however concentrations close to the surface were much greater (1.22 compared to 0.43 mM at 0.1 mbsf). Low micromolar concentrations of CH_4 were measured throughout the upper 3 m of sediment in upper muddy sediment strata, and were generally negligible below 3 mbsf in the sandy strata, suggesting oxidation in sandy sediments is occurring (Fig. 2.2 and 2.3). CH_4 concentrations were typically 2 to 3 times greater in VC2 compared to VC1, and CH_4 was negligible in the sandy reference core (Fig. 2.4). The presence of CH_4 in appreciable levels in VC1 and VC2, while being negligible in VC3, confirms that observed AT in seismic profiles are due to gas and that accumulation in shallow surface sediment in DBPF is occuring. The presence of CH-4 close to the sediment-water interface suggests that seepage, albeit in low amounts, is ongoing at DBPF. This is in agreement with previous observations (Szpak 2012a).

Groundwater discharge has been highlighted as a possible formation mechanism for pockmarks (Whiticar 2002; Christodolou et al., 2003), in particular in coastal settings. Groundwater discharge in the marine setting is driven by hydraulic gradients from coastal aquifers. In sandy high permeability settings groundwater may occur as submarine springs or seepage at the beach face (Holliday et al., 2007). Christodoulou et al. (2003) observed changes in salinity above pockmarks, together with constant water column methane profiles, to infer that seeping groundwater was the primary formation mechanism for pockmarks in the Corinth Gulf, Greece. A possible conduit for freshwater influx the DBPF is via permeable sandy strata and gravel deposits that characterise the shallow seabed in the region. However no such

deviation in Cl^- (data not shown) or SO_4^{2-} (Fig. 2.2 to 2.4) was observed. Together with previous water column salinity profiling (Szpak 2012a), these results support the conclusion that GD is not a formation mechanism for Dunmanus Bay pockmarks. However as noted by Szpak (2012a) periodic GD, such as in times of heavy rainfall, cannot be ruled out at present.

In the absence of observable freshwater influence, the rapid depletion of H_2S and CH_4 in sandy sediments (Fig. 2.2 and 2.3) suggests seawater influx may be occurring. This hypothesis is supported by the observation that SO_4^{2-} profiles increase to seawater levels from 1.27 mbsf in VC2 after initially reducing. Similar SO_4^{2-} trends were observed in a core from the 2009 survey, whereby SO_4^{2-} reduction was apparent in the first 1 m before increasing (Szpak 2012a). The presence of permeable sand and gravel layers may provide a conduit for the reintroduction of seawater from depth and oxidation of reduced chemical species. This may also be a possible mechanism for lateral migration of seeping gas from the below DBPF to surrounding sediments. This is one factor that might explain the observed subtle acoustic gas escape signatures (Szpak 2012a) and the low measured CH_4 concentrations on two separate surveys. Based on the multiple analysis performed here differences in lithology are a key parameter controlling the location of pockmarks in Dunmnaus Bay, the accumulation of gas and geochemical processes at the DBPF. Microbial and geochemical processes are discussed in more details in sections 2.3.2 and 2.3.3.

3.2 Distinct microbial activity and populations at the DBPF

NH_4^+ in sediment pore waters is derived from the microbial breakdown of marine and terrestrial organic nitrogen and is consumed in the microbial nitrification and denitrification processes that involve reduction of NO_3^- and NO_2^- to N_2. In anoxic, organic-rich marine sediments, the nitrogen transformation reactions cease at the conversion of organic nitrogen to NH_4^+ (Batley and Simpson 2009). NH_4^+ reach mM concentrations very close to the sediment water interface for VC2, which suggests a net flux to the water column and also significant degradative processes occurring. NH_4^+ displays linear increasing trends with depth for both VC1 and VC2 (Fig. 2.2 and 2.3). Close to the SWI NH_4^+ is 2.2 times greater at VC2 compared to VC1 (0.60 mM compared to 1.69 mM at 0.1 mbsf, respectively). NH_4^+ levels in VC2 were twice that of VC1 for the first 3 mbsf before approaching comparable levels in deeper sandy sediment strata (Fig. 2.2 and 2.3). VC3 displayed a distinct profile with much lower

NH_4^+ concentrations (Fig. 2.4). PO_4^{3-} in porewater reflects the microbial degradation of proteinaceous OM and also from microbial metabolism (released from ATP). PO_4^{3-} profiles for VC1 exhibited maximum concentrations around 0.7 mbsf to 1.22 mbsf, after a comparatively sharp increase from the SWI, while in contrast PO_4^{3-} profiles for VC2 exhibited maximum levels close to the SWI and an clear linear decreasing trend with depth (Fig. 2.3). These profiles indicate higher OM degradation rates and microbial activity in muddy sediments in DBPF, particularly at VC2.

Phospholipid fatty acids (PLFA) are of utility as a measure of viable sedimentary microbial biomass, both eukaryotic and bacterial (Guezennec and Fiala-Medioni 2006; Mills et al., 2006). PLFA analysis provide broad chemotaxonomic information, for example in determining the relative abundance of algal vs. bacterial biomass or the relative abundance of gram negative vs. gram positive bacteria (White et al., 1997). PLFAs ranged from up 0.80 μg g dw^{-1} at depths close to the surface, to very low concentrations in coarse sands in the deepest section of the cores (Fig. 2.2A). This trend reflects the particle size dependence of microbial biomass in marine sediments (Jackson and Weeks 2008). PLFA abundance was comparable between all three cores after 2.2 mbsf, but was 1.7 times higher in VC1 than VC2 and 2.7 times higher than VC3. PLFA's ranged from C_{14} to C_{24} carbons and were dominated by the $C_{16:0}$ (21.6 and 30.2%). Negligible polyunsaturated fatty acids (PUFA) were observed in samples downcore, indicating a low contribution of viable eukaryotic biomass in these cores.

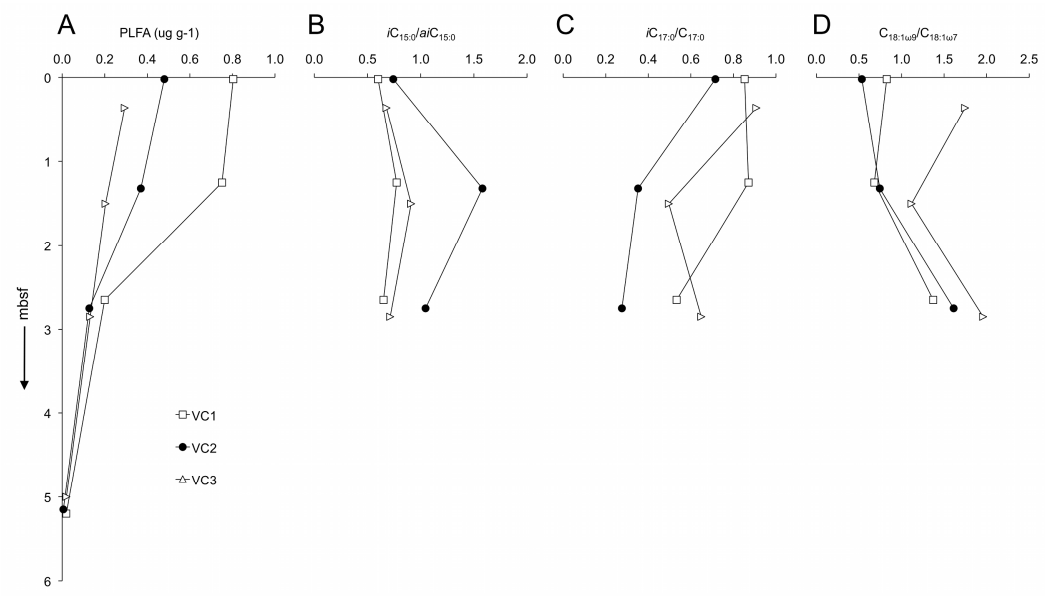

Figure 5: Downcore profiles of total phospholipid fatty acid (PLFA) abundances (A) and relevant PLFA ratios (B to D).

Gram-positive and anaerobic gram-negative bacteria primarily synthesize branched saturated fatty acids (brFA) while aerobic gram-negative bacteria are characterised by larger relative abundances of monounsaturated fatty acids (MUFA) (White et al., 1997). The ratio of brFA to MUFA was found to increase with depth initially in all cores, before decreasing again in sandy sediment. Assuming a predominantly bacterial source for MUFA in this setting (in the absence of PUFA), this likely reflects the increased abundance of gram-positive and anaerobic gram-negative bacteria with depth in muddy sulphidic sediments and the increased abundance of aerobic bacteria in sandy oxic sediments below muddy layers (and throughout VC3). Specific changes in relative abundances of populations within these groups are also likely and can be postulated based on relative changes in certain PLFAs. The ratio of $i\mathrm{C}_{12:0}$ to $ai\mathrm{C}_{12:0}$ was consistently higher in VC2 when compared to VC1 and VC3, in particular at 1.32 mbsf (Fig. 2.2B). The ratios of $i\mathrm{C}_{17:0}/\mathrm{C}_{17:0}$ and $\mathrm{C}_{18:1\omega9}/\mathrm{C}_{18:1\omega7}$ were also variable between cores and at different depths (Fig. 2.2C and D). Sulphate-reducing bacteria (SRB) have consistently higher ratios of $i\mathrm{C}_{12:0}$ to $ai\mathrm{C}_{12:0}$ (Dowling et al., 1986), which suggests that SRB are more prominent in VC2 compared to VC1 and VC3. This correlates with observed SO_4^{2-} reduction in this core (Fig. 2.3). In marine sediments $10\mathrm{MeC}_{16:0}$ has often been used as a diagnostic fatty acid for the *Desulfobacter* genera (Dowling et al., 1986; Rajendran et al., 1993), although its specificity may be questionable (Boschker et al., 2001). This fatty acid did not display comparable trends with $i\mathrm{C}_{12:0}/ai\mathrm{C}_{12:0}$. While being of limited taxonomic use these ratios do provide evidence of relative changes in bacterial populations between cores and with depth in the sediment column. Further evidence for the occurrence of distinct bacterial communities in DBPF was obtained from hierarchical cluster analysis (Fig. 2.6). Two major groupings were produced, whereby populations in muddy sediment strata in VC1 and VC2 clustered together and populations from deeper sandy strata and in VC3 clustered together. Inter-cluster similarity was less than 20%. Sub-groupings were evident also, whereby populations at the surface and 1.3 mbsf in VC1 displayed 92% similarity to each other and the corresponding depths in VC2 were 84% similar.

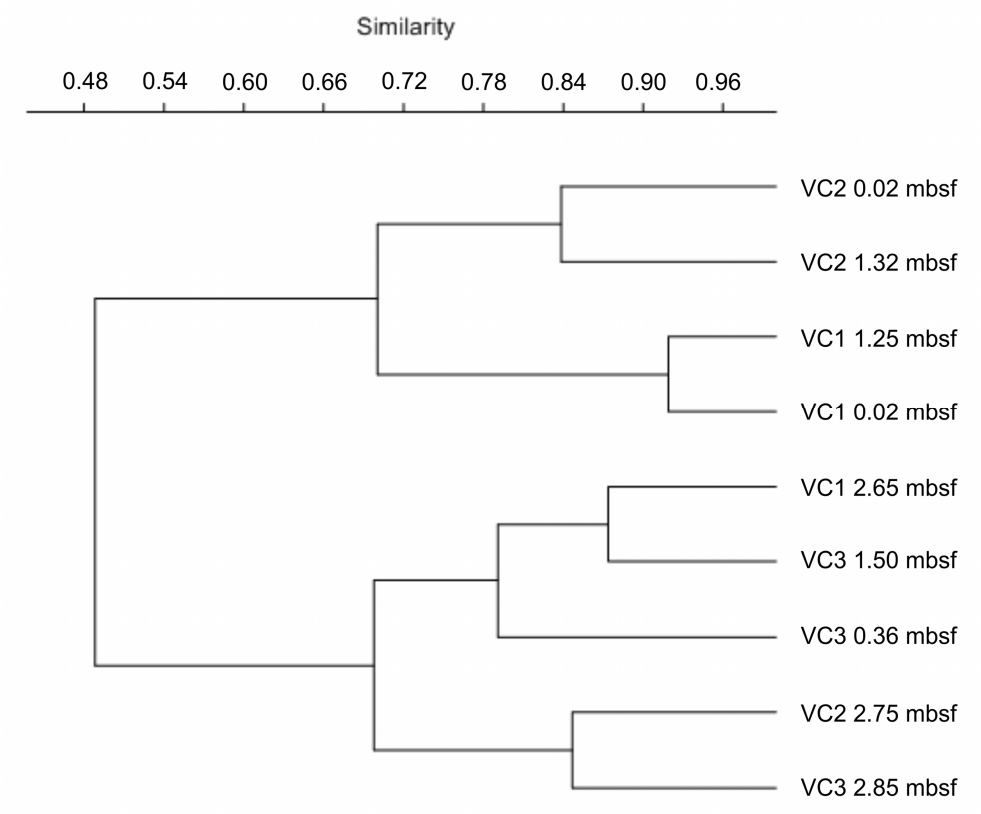

Figure 6: Hierarchical cluster analysis of PLFA profiles using the Bray-Curtis similarity matrix.

Cluster analysis of digitized DGGE lanes supports the conclusions drawn from PLFA interpretation. Fig. 2.7 indicates that bacterial populations close to the surface and at about 1 mbsf in VC1 and VC2 display 72% similarity. The near-surface bacterial population in VC3 displays the highest species richness based on the number of bands present, while in comparison the cores within DBPF exhibit lower richness. The near-surface bacterial community is only 32% similar to all other samples. Whether these observed changes change in bacterial biomass abundance and community structure is related primarily to lithological differences, or whether this as a result of seepage activity in the pockmark field cannot be distinguished at present. Population diversity may be expected to decrease in an active seepage setting, in particular with the presence of toxic by-products such as H_2S, such as observed here. Archaeal diversity, based on analysis of samples from 1 mbsf (including a control core GC14) is low and indicates a very similar archaeal community structure within DBPF, and one that this is very similar to sediment outside the pockmark field (Fig. 2.8). Archaeal biomarkers, (e.g. archaeol, crocetane and pentamethyl-eicosane) were not observed in neutral lipid fractions from these cores (data not shown). This suggests that archaea

may play a minor role in ongoing processes at DBPF and that existing populations likely belong to extant groups in this setting rather than distinct seepage-affiliated phylotypes.

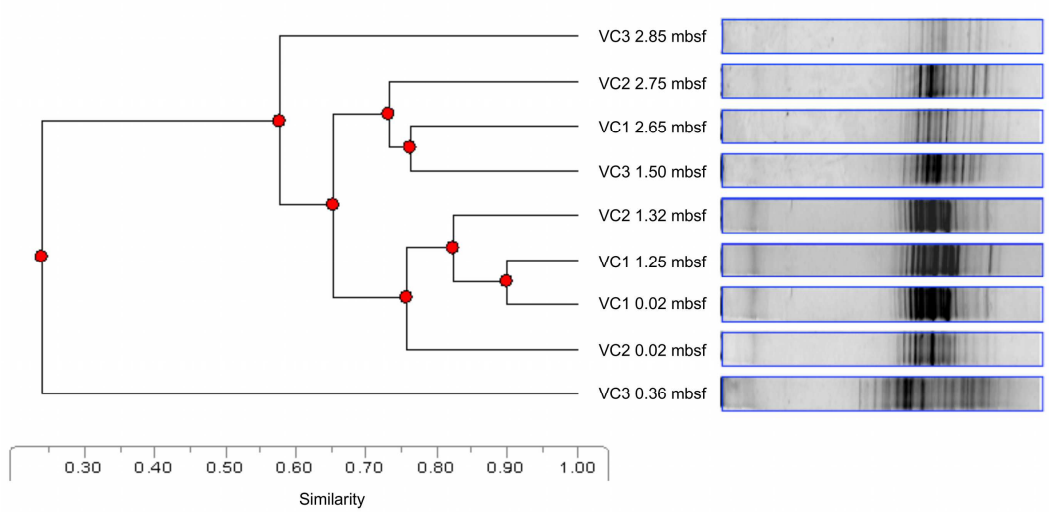

Figure 7: 16S rRNA bacterial denaturing gradient gel electrophoresis (DGGE) profiles and hierarchical cluster analysis.

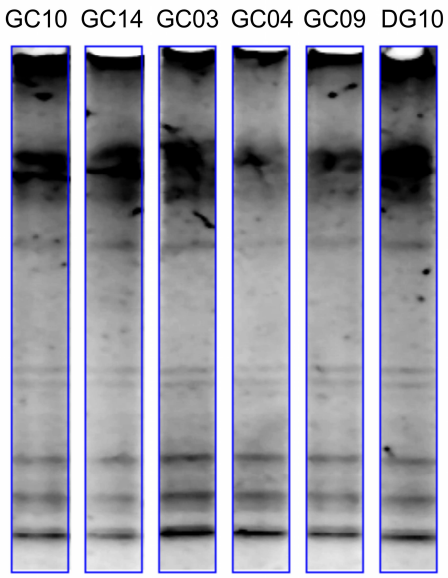

Figure 8: 16S rRNA archaeal denaturing gradient gel electrophoresis profiles of samples from the survey in 2009. Sampling depth for DGGE analysis was 1 mbsf. See Fig. 2.1 for locations. GC14 is the control core, taken from outside the pockmark field.

1D ^{1}H-NMR analysis of NaOH extracts allow an overview of total OM composition and specific regions can be assigned to molecular classes in complex environmental

samples (Kelleher and Simpson 2006; Simpson et al., 2007; Simpson et al., 2011; McCaul et al., 2011; Spence et al., 2011; Szpak et al., 2012b). Protons bonding to aliphatic compounds were identified (0.72 to 1.9 ppm) as well as protons associated with carbohydrates and O-alkyl groups on amino acids (3.2 and 4.2 ppm) (Fig. 2.9). Based on the broad unresolved peak from 0.8 to 4.4 ppm, OM is greater in VC1 and VC2 in muddy sediment strata, compared to VC3 and in deeper sandy strata. This is reflected in bulk LOI profiles (Fig. 2.2 to and 2.3). The amount of labile OM, based on the region characteristic of carbohydrates, decreases significantly from the surface to ~ 1 mbsf in both VC1 and VC2, while only slight differences were observed for VC3. This suggests significant microbial degradation of OM and supports conclusion drawn from pore water geochemistry. Protons associated with the *N*-acetylmuramic acid were based on the characteristic resonance peak for the *N*-acetyl functional group at 2.03 ppm, as previously described (Simpson et al., 2007; Szpak et al., 2012b). *N*-acetylmuramic acid is one of the primary constituents composing the bacterial cell wall polymer, peptidoglycan. Peptidoglycan was therefore a significant component of sedimentary OM in most samples and indicates a substantial contribution of bacteria-derived OM in these sediments. Peptidoglycan typically represents about 90 % of dry cell weight of Gram-positive bacteria and on average only 10% of dry cell weight of Gram-negative bacteria. However Gram-negative bacteria are typically most abundant in both oxic (Hagström et al., 2000) and anoxic marine environments (Moriarty and Hayward 1982). Thus most peptidoglycan in marine settings is probably derived from Gram-negative cell walls (Pedersen et al., 2001). In muddy strata the relative contribution of peptidoglycan appears to be greater in VC2 compared to VC1, while both are higher than VC3. This reflects an increased abundance of bacterial-derived OM in VC2. Since PLFA analysis has shown that the abundance of viable bacteria, is greater in VC1 compared to VC2 (Fig. 2.2), it is likely that much of the peptidoglycan in VC2 could be derived from microbial necromass. Another possible source is from depositional input rather than *in situ* production as this polymer is chemically recalcitrant and a significant component of soil (Simpson et al., 2007), marine particulate (Benner and Kaiser 2003), refractory dissolved OM (McCarthy et al., 1998; Benner and Kaiser 2003; McCaul et al., 2011) and marine sedimentary OM (Pedersen et al., 1990; Szpak et al., 2012b).

Direct NMR of pore water using has to our knowledge not been performed on sediment pore waters, and has significant potential for elucidating microbially

mediated reactions between sedimentary aqueous and solid phases. 1D water suppressed ^{1}H NMR spectra for selected depths from each core are given in Fig. 2.10. Pore water DOM should correspond to both high molecular weight and low molecular weight products of depolymerisation of detrital OM (Burdige 2007). The broad unresolved peak from 0.8 to 4.2 ppm reflects the amount of complex DOM and comparison between cores indicates highest relative abundance of total DOM in VC1 and VC2 in the first 1 m approximately. This amount of DOM is comparable between cores in sandy strata. This correlates with the increased microbial activity and OM degradation observed from pore water NH_4^+ and PO_4^{3-}. A range of volatile organic acids and microbial metabolic end-products were identified in porewater ^{1}H NMR spectra (Fig. 2.10). Specific assignments were leucine (1), ethanol (2), lactic acid (3), acetic acid (4), dimethyl sulphide (2), acetone (6), pyruvic acid (7), methanol (8), glycerol (9), Tyrosine, phenylalanine and formic acid (not shown). Volatile organic acids such as acetic acid, formic acid, lactic acid and pyruvic acid are considered important intermediate products of the anaerobic metabolism of higher molecular weight organics (carbohydrates, fatty acids and proteins) to CH_4 and CO_2 (Sansone and Martens 1982; Finke et al., 2007a). Acetic acid is thought to be the primary organic substrate for sulphate reducing bacteria (Sørensen et al., 1981). These volatile organic are significant components of porewater DOM and in highest relative abundance in porewater from muddy strata in VC1 and VC2 and in agreement with pore water geochemistry, indicate significant anaerobic degradation OM in the first 1 m of sediment in both VC1 and VC2. The occurrence of dimethyl sulphide (DMS) and methanol are discussed in detail in section 2.3.3.

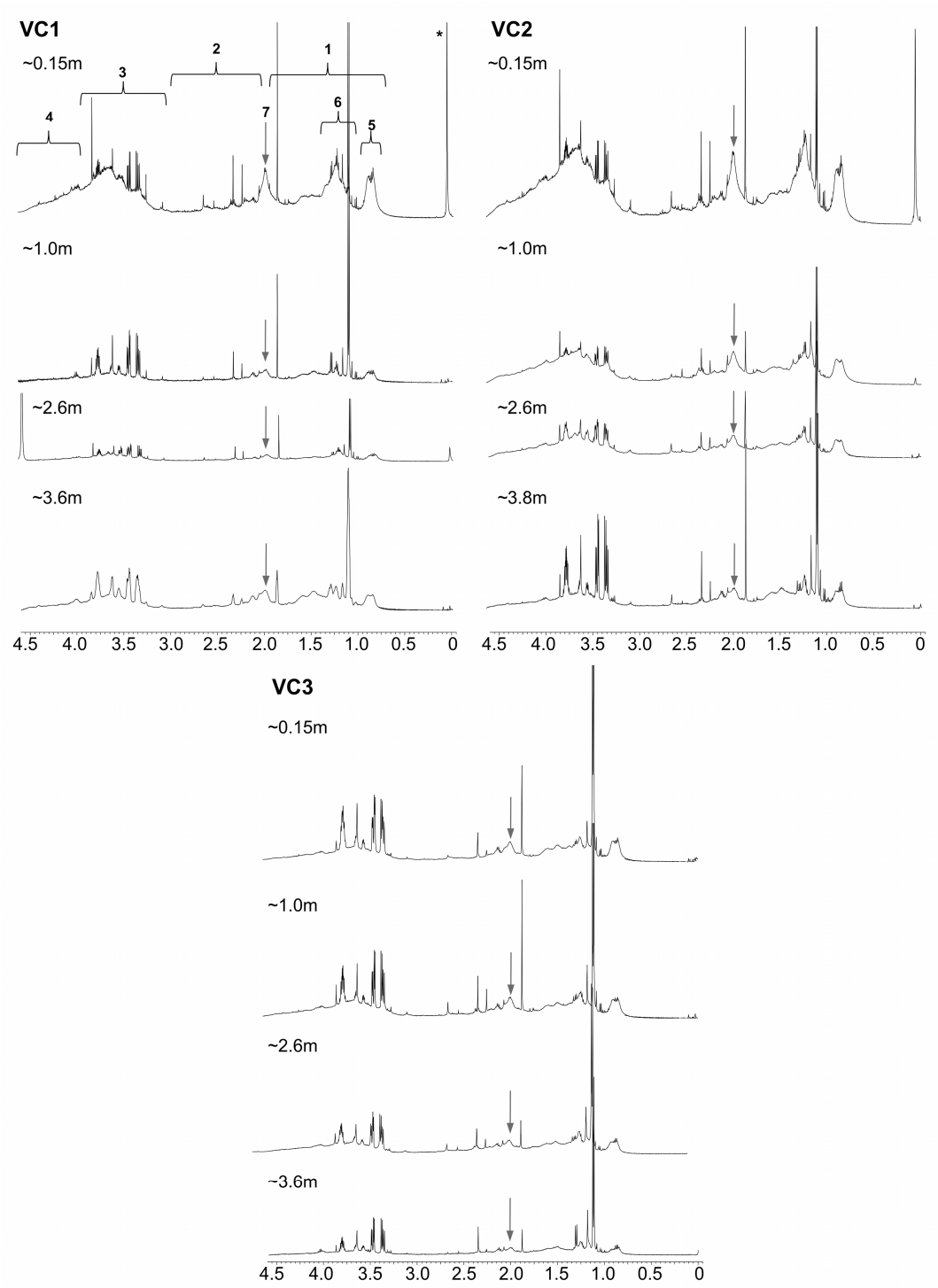

Figure 9: 1D ^{1}H NMR spectra (0 to 4.2 ppm region) obtained from NaOH extracts. General region assignments correspond to aliphatics (1), ?? (2), carbohydrates and amino acids (3), anomeric carbon (4). More specific assignments are protons associated with CH_3 groups in amino acid side chains (2), protons associated with methylene groups in aliphatic compounds (6), protons associated with N-acetyl functional groups in peptidoglycan (7) and protons associated with naturally occurring silicates compounds (*). The grey arrow highlights the resonance peak associated with peptidoglycan.

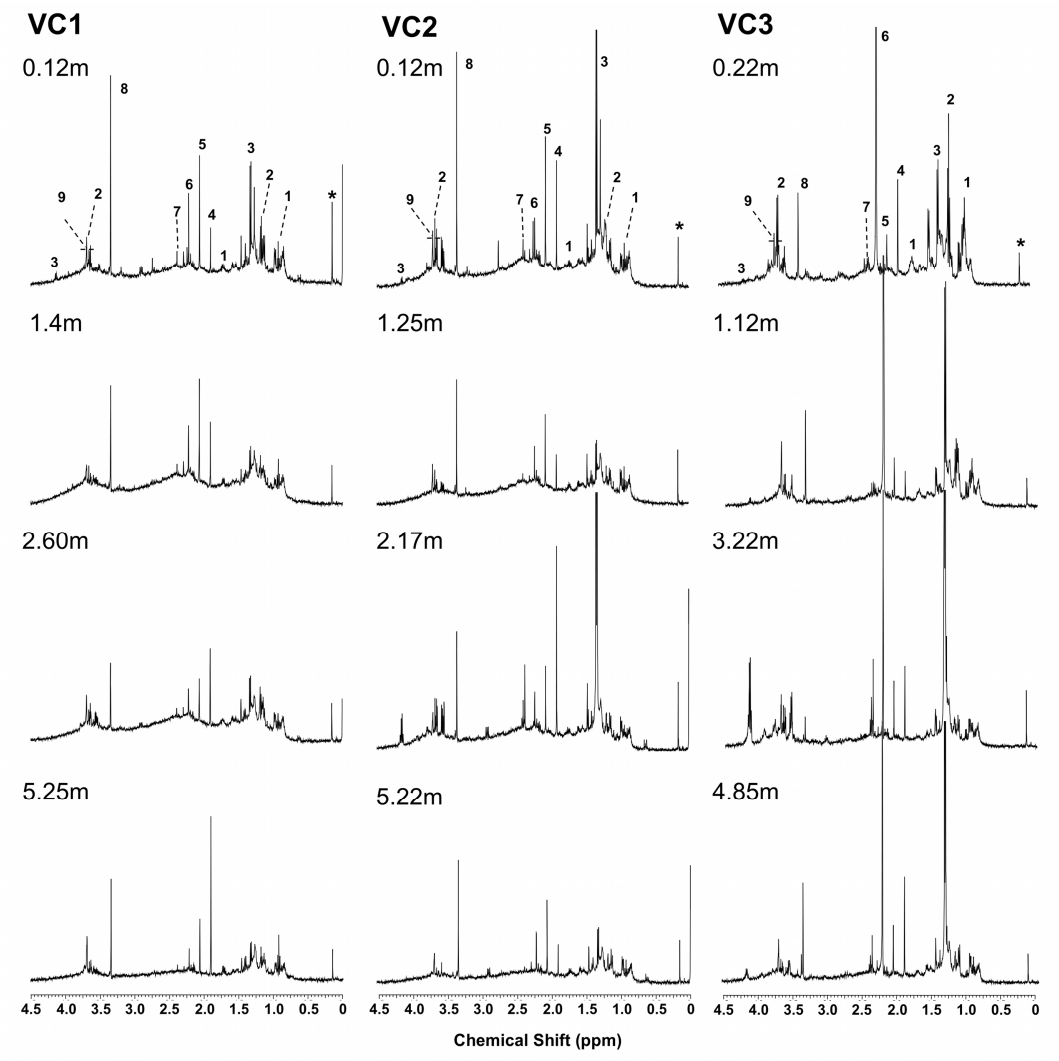

Figure 10: 1D water-suppressed ^{1}H NMR spectra of porewater dissolved organic matter from selected depths in VC1, VC2 and VC3. Specific assignments correspond to leucine (1), ethanol (2), lactic acid (3), acetic acid (4), dimethyl sulphide (2), acetone (6), pyruvate (7), methanol (8) and glycerol (9). Tyrosine, phenylalanine and formate were also identified in the 6.8 to 8.2 ppm region but are not included for clarity.

The results presented here confirm that distinct bacterial populations are present in muddy surface layers in acoustically turbid pockmarked and non-pockmarked sediment in DBPF. Distinct variation in overall community composition has been observed based on relative changes in bacterial PLFAs, whereby anaerobic bacteria appear to be in highest abundance in VC2. The occurrence and increased relative abundance of peptidoglycan in these sediments relative to VC3 indicates an increased contribution of bacterial-derived OM, in particular in VC2. Peptidoglycan signals most likely reflect significant bacterial necromass and/or depositional input, rather

than viable bacterial biomass. Comparison of NH_4^+ and PO_4^{3-} pore water profiles and pore water DOM indicate that microbial activity and OM degradation is enhanced in muddy sediments in VC1 and VC2, and that this is enhanced in non-pockmarked gassy sediments in DBPF (VC2).

3.3 Evidence for alternative sources of gas?

SO_4^{2-} reduction and H_2S production in marine sediments is generally linked, whereby the utilization of SO_4^{2-} as an electron acceptor in OM mineralization yields reduced H_2S (Jørgensen 1982). H_2S is typically precipitated as pyrite or else reoxidised to SO_4^{2-}. The presence of significant levels H_2S in VC1 and VC2 in the absence of SO_4^{2-} depletion (Fig. 2.2 and 2.3) are atypical and indicates there must be an alternative source of H_2S. In all cores fine-grained muddy strata were dominated by olive-green to grey sediment and did not exhibit highly reduced grey/black sediments typical of pyrite precipitation. Numerous layers with significant high densities shell hash and organic material was observed throughout the first 2 m of sediment in both VC1 and VC2. These layers were also characterised by horizontal cracking and strong sulphide odours. These coincide in a number of cases with spikes in H_2S levels (Fig. 2.3). Hence these layers organic-rich shelly layers are a potential source of H_2S. A possible explanation for the presence of mM concentrations of H_2S in the presence of SO_4^{2-} is the anaerobic decomposition of the sulphur-containing proteinaceous OM (Dunnette et al., 1982). In the marine environment algal and macrophyte decomposition is the most common source of proteinaceous OM (Fry 1987).

There is evidence that there is considerable input from dead and decaying biomass in DBPF. During the CV09_23 survey in 2009 a dark-coloured organic-rich sample was retrieved from a boxcore from within a pockmark cluster in the northeast of the field (Fig. 2.1, BG10). This sample had distinct putrefying odour. PLFAs were dominated by very high abundances of C_{20}, C_{22} and C_{24} polyunsaturated fatty acids, which are likely derived from eukaryotic biomass such as micro- or macroalgae (Volkman 2006). Sterols profiles were also distinct, whereby $C_{29}\Delta^{2,24(28)}$ (fucosterol) and its isomers (Δ_2- and Δ_7-avenasterol) were present in much higher abundance compared to commonly major sterols (e.g. $C_{27}\Delta^2$ and $C_{29}\Delta^2$). $C_{29}\Delta^{2,24(28)}$ sterols are typically the major sterols in Phaeophyceae (brown algae) (Patterson 1971). Therefore the sediment within this pockmark was composed a significant component fresh and decaying macroalgal OM, probably kelp or seaweed.

DMS was identified as a major component in porewater DOM in most sub-samples analysed, in particular in muddy strata in VC1 and VC2 (Fig. 2.10). DMS (along with methanthiol) is a significant volatile component of the organic sulphur cycle and one of the most common gaseous compounds emitted from coastal marine environments (Bates et al., 1992). The major source of DMS is from degradation of organo-sulphur compounds such as dimethylsulfoniopropionate (DMSP) or sulphur-containing amino acids (Kiene 1988; Taylor and Kiene 1989), or from methylation of H_2S (Finster et al., 1990). DMSP is an osmolyte found in macroalgal (Sørensen 1988) and halophilic higher plants (Finster et al., 1990). Microbial degradation of DMS and methanethiol produces CO_2 and CH_4, whereby in high concentrations CH_4 is favoured and in low concentrations CO_2 is favoured (Lyimo et al., 2009). It has also been proposed that their degradation in freshwater environments is mediated by methanogenic archaea, and predominantly produces CH_4, while in marine environments both SRB and methanogenic archaea are involved, with CO_2 being the dominant product (Lomans et al., 1997). This provides a clear potential metabolic route for the *in-situ* production of CH_4 in low amounts, and in the presence of SO_4^{2-}. Further evidence for a source of H_2S, other than from SO_4^{2-} reduction was obtained from analysis of amplified and sequenced dominant bands from DGGE gels (2009 survey, data not shown). A major band present at 1 mbsf in DBPF, and which was not observed in a control core (GC14) was closely related (99%) to *Dethiobacter* sp. The model representative from this genus, *Dethiobacter alkaliphilus*, is an obligately anaerobic non-sulphate reducing representative of the reductive sulphur cycle (Sorokin 2008).

In the presence of SO_4^{2-}, SRB typically outcompete methanogens for substrates such as acetate or H_2 (Jørgensen 1982). However it has been shown that non-competitive substrates may be utilised by methanogens and allow methanogenesis and sulphate reduction simultaneously (Oremland and Polcin 1982a). This has been demonstrated in a number of settings including anoxic salt marsh sediments (Oremland et al., 1982b), estuarine sediments (Oremland and Polcin 1982a), in continental margin carbonate sediments (Mitterer et al., 2001), active mud volcanos (Lazar et al., 2012). In addition it has been observed that appreciable levels of CH_4 occur in SO_4^{2-} rich sediments in about one sixth of all Deep Sea Drilling Project and Ocean Drilling Project open ocean sites (D'Hondt et al., 2002). To main non-competitive substrates known are methanol, methylamine and trimethylamine (King et al., 1983; King 1984; Finke et al., 2007b). Methanol was a major compound

in porewater DOM from VC1 and VC2, in particular in the first 1 m of sediment (Fig. 2.9). Therefore there is enough evidence to hypothesis that *in situ* production of CH_4 is occurring in DBPF via non-competitive substrate utilization.

Assuming that the observed AT in Fig. 2.1 reflects the distribution of gas in the sediment column, it appears that gas is present in a relatively shallow layer in the first 2 m of sediment. No AT or other associated gas signatures were observed below these depths, although overlying gas and the gravel deposits could have caused signal starvation. This AT region correlates well with measured CH_4 concentrations in both VC1 and VC2. Gas is present either as a result of migration from depth or alternatively is produced *in situ*, or it may be a combination of both. The peak in CH_4 between 1.4 and 2.0 mbsf (highlighted in red in Fig. 2.3) suggest that *in situ* production is occurring at these depths. Interestingly this region correlates well with the observed peak in total OM content, and suggests that OM degradation has a role in CH_4 production. It could be a by-product of OM degradation via DMSP and DMS. DMS is an important gaseous compound in coastal settings and could itself be a source of gas in the DBPF. Microbial production of CH_4 via DMS metabolism is also possible. Thus there appears to be multiple lines of evidence to suggest that *in situ* production of CH_4 is occurring in DBPF. The outlined processes are therefore possible mechanisms for gas production and pockmark formation, in particular in shallow coastal settings and bays. If this were the case this would represent the first link between these biogeochemical processes and seabed fluid flow and pockmark formation.

4 Conclusions

Particle size profiles and sediment type within the DBPF exhibited clear stratification with depth, whereby fine-grained sediment is succeeded by progressively coarser strata. The occurrence of fine-grained sandy mud and mud appears to be localized to DBPF and thus this characteristic lithology may account for the pockmark formation within DBPF and not in surrounding sediment. The occurrence of low concentrations of CH_4 in sediments strata where SO_4^{2-} was not depleted suggests that CH_4 migration from depth may be occurring. However evidence presented here also indicates *in-situ* production of volatile compounds such as DMS, as well as CH_4 are a possible source of gas. CH_4 production via non-competitive substrate utilization of methanol may be occurring as well as the production of CH_4 (and CO_2) from microbial reduction of volatile sulphur compounds such as DMS. This is supported by the atypical pore water profiles whereby significant concentrations of CH_4 and H_2S are observed in the presence of SO_4^{2-}. A possible source for DMS and H_2S is from putrefactive degradation of proteinaceous macroalgal OM. Bacterial activity appears to be higher within the DBPF, and in particular microbial activity appears to be greater in non-pockmarked acoustically turbid sediment. The effect of underlying permeable sands and gravel on gas migration and fate, as well as other factors such as tidal and hydrographic regime, and ground water escape remain a distinct unknown at present.

5 References

Bates T, Lamb B, Guenther A, Dignon J, Stoiber R. 1992. Sulfur emissions to the atmosphere from natural soures. J Atmos Chem 1992 14(1):312-337.

Batley GE, Simpson SL. 2009. Development of guidelines for ammonia in estuarine and marine water systems. Mar Pollut Bull 28(10):1472-1476.

Benner R, Kaiser K. 2003. Abundance of amino sugars and peptidoglycan in marine particulate and dissolved organic matter. Limnol Oceanogr 118-128.

Boschker H, Graaf W, Köster M, Meyer□Reil LA, Cappenberg T. 200. Bacterial populations and processes involved in acetate and propionate consumption in anoxic brackish sediment. FEMS Microbiol Ecol 32(1):97-103.

Boudreau BP, Huettel M, Forster S, Jahnke RA, McLachlan A, Middelburg JJ, et al. 2001. Permeable marine sediments: overturning an old paradigm. Eos, Transactions American Geophysical Union 82(11):133-136.

Burdige DJ. 2007 Preservation of organic matter in marine sediments: controls, mechanisms, and an imbalance in sediment organic carbon budgets? Chem Rev 107(2):467- 482.

Christodoulou D, Papatheodorou G, Ferentinos G, Masson M. 2003. Active seepage in two contrasting pockmark fields in the Patras and Corinth gulfs, Greece. Geo-Mar Lett 23(3):194-199.

D'Hondt S, Rutherford S, Spivack AJ. 2002. Metabolic activity of subsurface life in deep-sea sediments. Science 292(2262):2067-2070.

Dowling NJE, Widdel F, White DC. 1986. Phospholipid ester-linked fatty acid biomarkers of acetate-oxidizing sulphate-reducers and other sulphide-forming bacteria. J Gen Microbiol 132(7):1812-1822.

Dunnette DA, Chynoweth DP, Mancy KH. 1982. The source of hydrogen sulfide in anoxic sediment. Water Res 19(7):872-884.

Fader GBJ. 1991. Gas-related sedimentary features from the eastern Canadian continental shelf. Cont Shelf Res 11(8):1123-1123.

Finke N, Vandieken V, Jørgensen BB. 2007a. Acetate, lactate, propionate, and isobutyrate as electron donors for iron and sulfate reduction in Arctic marine sediments, Svalbard. FEMS Microbiol Ecol 29(1):10-22.

Finke N, Hoehler TM, Jørgensen BB. 2007b. Hydrogen 'leakage' during methanogenesis from methanol and methylamine: implications for anaerobic carbon degradation pathways in aquatic sediments. Environ Microbiol 9(4):1060-1071.

Finster K, King GM, Bak F. 1990. Formation of methylmercaptan and dimethylsulfide from methoxylated aromatic compounds in anoxic marine and fresh water sediments. FEMS Microbiol Lett 74(4):292-301.

Fry J. 1987. Functional roles of major groups of bacteria associated with detritus. In: Moriarty DJW and Pullin RSV (eds.) Detritus and microbial ecology in aquaculture. INCLARM Conference Proceedings: Philippines p83-122.

Garcia-Gil S. 2003. A natural laboratory for shallow gas: the Rías Baixas (NW Spain). Geo-Mar Lett 23(3):212-229.

Garcia-Gil S, Vilas F, Garcia-Garcia A. 2002. Shallow gas features in incised-valley fills (Rıa de Vigo, NW Spain): a case study. Cont Shelf Res 22(16):2303-2312.

Gay A, Lopez M, Ondreas H, Charlou JL, Sermondadaz G, Cochonat P. 2006. Seafloor facies related to upward methane flux within a Giant Pockmark of the Lower Congo Basin. Mar Geol 226(1):81-92.

Gonçalves CN, Dalmolin RSD, Dick DP, Knicker H, Klamt E, Kögel-Knabner I. 2003. The effect of 10% HF treatment on the resolution of CPMAS ^{13}C NMR spectra and on the quality of organic matter in Ferralsols. Geoderma 116(3):373-392.

Grasshoff K, Ehrhardt M, Kremling K, Almgren T. 1983. Methods of seawater analysis. : Wiley Online Library

Guezennec J, Fiala□Medioni A. 2006. Bacterial abundance and diversity in the Barbados Trench determined by phospholipid analysis. FEMS Microbiol Ecol 19(2):83-93.

Hagström Ä, Pinhassi J, Zweifel UL. 2000. Biogeographical diversity among marine bacterioplankton. Aquat Microb Ecol 21(3):231-244.

Harrington P. 1982. Formation of pockmarks by pore-water escape. Geo-Mar Lett 2(3):193-197.

Holliday D, Stieglitz T, Ridd P, Read W. 2007. Geological controls and tidal forcing of submarine groundwater discharge from a confined aquifer in a coastal sand dune system. J Geophys Res: Oceans 112:1-10.

Hovland M, Judd A. 1988. Seabed pockmarks and seepages: impact on geology, biology, and the marine environment. Springer.

Huettel M, Røy H, Precht E, Ehrenhauss S. 2003. Hydrodynamical impact on biogeochemical processes in aquatic sediments. Hydrobiologia 494(1):231-236.

Huettel M, Rusch A. 2000. Transport and degradation of phytoplankton in permeable sediment. Limnol Oceanogr 234-249.

Huettel M, Ziebis W, Forster S, Luther G. 1998. Advective transport affecting metal and nutrient distributions and interfacial fluxes in permeable sediments. Geochim Cosmochim Acta 62(4):613-631.

Jackson CR, Weeks AQ. 2008. Influence of particle size on bacterial community structure in aquatic sediments as revealed by 16S rRNA gene sequence analysis. Appl Environ Microbiol 74(16):2237-2240.

Jørgensen BB. 1982. Mineralization of organic matter in the sea bed—the role of sulphate reduction. Nature 296:643-642.

Judd A, Hovland M. 2007. Seabed fluid flow: the impact on geology, biology and the marine environment. Cambridge University Press.

Kelleher BP, Simpson AJ. 2006. Humic substances in soils: Are they really chemically distinct? Environ Sci Technol 40(12):4602-4611.

Kelley JT, Dickson SM, Belknap DF, Barnhardt WA, Henderson M. 1994. Giant sea-bed pockmarks: evidence for gas escape from Belfast Bay, Maine. Geology 22(1):29-62.

Kiene RP. 1988. Dimethyl sulfide metabolism in salt marsh sediments. FEMS Microbiol Lett 23(2):71-78.

King GM. 1984. Utilization of hydrogen, acetate, and “noncompetitive”; substrates by methanogenic bacteria in marine sediments. Geomicrobiol J 3(4):272-306.

King GM, Klug M, Lovley D. 1983. Metabolism of acetate, methanol, and methylated amines in intertidal sediments of Lowes Cove, Maine. Appl Environ Microbiol 42(6):1848-1823.

Knebel HJ, Scanlon KM. 1982. Sedimentary framework of Penobscot Bay, Maine. Mar Geol 62(3):302-324.

Lam B, Simpson AJ. 2007. Direct 1H NMR spectroscopy of dissolved organic matter in natural waters. Analyst 133(2):263-269.

Lazar CS, John Parkes R, Cragg BA, L'Haridon S, Toffin L. 2012. Methanogenic activity and diversity in the centre of the Amsterdam Mud Volcano, Eastern Mediterranean Sea. FEMS Microbiol Ecol 81(1):243-224

Lomans BP, Smolders A, Intven LM, Pol A, Op D, Van Der Drift C. 1997. Formation of dimethyl sulfide and methanethiol in anoxic freshwater sediments. Appl Environ Microbiol 63(12):4741-4747.

Lyimo TJ, Pol A, Harhangi HR, Jetten MSM, Op den Camp HJM. 2009. Anaerobic oxidation of dimethylsulfide and methanethiol in mangrove sediments is dominated by sulfate□reducing bacteria. FEMS Microbiol Ecol 70(3):483-492.

MacCarthy IAJ. 2007. The South Munster Basin of southwest Ireland. J Maps 3(1):149-172.

McCarthy MD, Hedges JI, Benner R. 1998. Major bacterial contribution to marine dissolved organic nitrogen. Science 281(2374):231-234.

McCaul MV, Sutton D, Simpson AJ, Spence A, McNally DJ, Moran BW, et al. 2011. Composition of dissolved organic matter within a lacustrine environment. Environ Chem 8(2):146-124.

Mills CT, Dias RF, Graham D, Mandernack KW. 2006. Determination of phospholipid fatty acid structures and stable carbon isotope compositions of deep-sea sediments of the Northwest Pacific, ODP site 1179. Mar Chem 98(2):197-209.

Mitterer RM, Malone MJ, Goodfriend GA, Swart PK, Wortmann UG, Logan GA, et al. 2001. Co-generation of hydrogen sulfide and methane in marine carbonate sediments. Geophys Res Lett 28(20):3931-3934.

Monteys X, Bloomer S, Chapman R. 2010. Multi-frequency acoustic seabed characterisation in shallow gas-bearing sediments in Dunmanus Bay, SW Ireland. Geophysical Research Abstracts 12, EGU2010-10707-2, EGU General Assembly, Vienna

Moriarty D, Hayward A. 1982. Ultrastructure of bacteria and the proportion of Gram-negative bacteria in marine sediments. Microb Ecol 8(1):1-14.

Nelson H, Thor D, Sandstrom M, Kvenvolden K. 1979. Modern biogenic gas-generated craters (sea-floor “pockmarks”) on the Bering Shelf, Alaska. Geological Society of America Bulletin 90(12):1144-1122.

Oremland RS, Polcin S. 1982a. Methanogenesis and sulfate reduction: competitive and noncompetitive substrates in estuarine sediments. Appl Environ Microbiol 44(6):1270-1276.

Oremland RS, Marsh LM, Polcin S. 1982b. Methane production and simultaneous sulphate reduction in anoxic, salt marsh sediments. Nature 296:143-142.

Patterson GW. 1971. The distribution of sterols in algae. Lipids 6(2):120-127.

Paull C, Ussler III W, Maher N, Greene H, Rehder G, Lorenson T, et al. 2002. Pockmarks off Big Sur, California. Mar Geol 181(4):323-332.

Paull C, Ussler III W, Borowski W. 1999. Freshwater ice rafting: an additional mechanism for the formation of some high-latitude submarine pockmarks. Geo-Mar Lett 19(1):164-168.

Pedersen AGU, Thomsen TR, Lomstein BA, Jorgensen NOG. 2001. Bacterial influence on amino acid enantiomerization in a coastal marine sediment. Limnol Oceanogr 46(6):1328-1369.

Pickrill R. 2006. Shallow seismic stratigraphy and pockmarks of a hydrothermally influenced lake, Lake Rotoiti, New Zealand. Sedimentology 40(2):813-828.

Rajendran N, Suwa Y, Urushigawa Y. 1993. Distribution of phospholipid ester-linked fatty acid biomarkers for bacteria in the sediment of Ise Bay, Japan. Mar Chem 42(1):39-26.

Rogers JN, Kelley JT, Belknap DF, Gontz A, Barnhardt WA. 2006. Shallow-water pockmark formation in temperate estuaries: A consideration of origins in the western gulf of Maine with special focus on Belfast Bay. Mar Geol 222(1):42-62.

Sansone FJ, Martens CS. 1982. Volatile fatty acid cycling in organic-rich marine sediments. Geochim Cosmochim Acta 46(9):1272-1289.

Santos IR, Eyre BD, Huettel M. 2011. The driving forces of porewater and groundwater flow in permeable coastal sediments: A review. Estuar Coast Shelf Sci 98:1-12.

Simpson AJ, Brown SA. 2002. Purge NMR: effective and easy solvent suppression. J Magn Reson 172(2):340-346.

Simpson AJ, McNally DJ, Simpson MJ. 2011. NMR spectroscopy in environmental research: from molecular interactions to global processes. Prog Nucl Magn Reson Spectrosc 28(3):97-172.

Simpson AJ, Simpson MJ, Smith E, Kelleher BP. 2007. Microbially derived inputs to soil organic matter: are current estimates too low? Environ Sci Technol 41(23):8070-8076.

Sørensen J. 1988. Dimethylsulfide and methane thiol in sediment porewater of a Danish estuary. Biogeochemistry 6(3):201-210.

Sørensen J, Christensen D, Jørgensen BB. 1981. Volatile fatty acids and hydrogen as substrates for sulfate-reducing bacteria in anaerobic marine sediment. Appl Environ Microbiol 42(1):2-11.

Sorokin DY, Tourova T, Mußmann M, Muyzer G. 2008. *Dethiobacter alkaliphilus* gen. nov. sp. nov., and *Desulfurivibrio alkaliphilus* gen. nov. sp. nov.: two novel representatives of reductive sulfur cycle from soda lakes. Extremophiles 12(3):431-439.

Spence A, Simpson AJ, Mcnally DJ, Moran BW, McCaul MV, Hart K, et al. 2011. The degradation characteristics of microbial biomass in soil. Geochim Cosmochim Acta 72(10):2271-2281.

Szpak M. 2012a. Chemical and physical dynamics of marine pockmarks with insights into the organic carbon cycling on the Malin Shelf and in the Dunmanus Bay, Ireland.

Szpak M, Monteys X, O'Reilly S, Simpson A, Garcia X, Evans RL, et al. 2012b. Geophysical and geochemical survey of a large marine pockmark on the Malin Shelf, Ireland. Geochem Geophy Geosy 13(1):1-18.

Taylor BF, Kiene RP. 1989. Microbial metabolism of dimethyl sulfide. Biogenic sulfur in the environment. ACS Symposium Series: ACS Publications.

Ussler W, Paull CK, Boucher J, Friederich G, Thomas D. 2003. Submarine pockmarks: a case study from Belfast Bay, Maine. Mar Geol 202(3):172-192.

Volkman JK. Lipid markers for marine organic matter. Marine Organic Matter: Biomarkers, Isotopes and DNA 2006, p.27-70.

White DC, Ringelberg DB. 1998. Signature lipid biomarker analysis. Techniques in microbial ecology.Oxford University Press, New York, NY p.222-272.

White DC, Ringelberg DB, Macnaughton SJ, Srinivas A, David S. 1997. Signature Lipid Biomarker Analysis for Quantitative Assessment In Situ of Environmental Microbial Ecology. American Chemical Society. p 22.

Whiticar MJ. 2002. Diagenetic relationships of methanogenesis, nutrients, acoustic turbidity, pockmarks and freshwater seepages in Eckernförde Bay. Mar Geol 182(1):29-23.

Wilson AM, Huettel M, Klein S. 2008. Grain size and depositional environment as predictors of permeability in coastal marine sands. Estuar Coast Shelf Sci 80(1):193-199.

Wu D, Chen A, Johnson CS. 1992. An improved diffusion-ordered spectroscopy experiment incorporating bipolar-gradient pulses. J Magn Reson A 112(2):260-264.